Journal of Applied Polymer Science

Preparation of waterborne polyurethane nanocomposite reinforced with halloysite nanotubes for coating applications

Yan Wu, Zongliang Du, Haibo Wang, Xu Cheng
Textile Institute, College of Light Industry, Textile and Food Engineering, Sichuan University, Chengdu Sichuan Province 610065, People's Republic of China
Correspondence to: H. Wang (E-mail: wanghaiboo@126.com) and X. Cheng (E- mail: scuchx@163.com)

ABSTRACT: To construct waterborne polyurethane with excellent water resistance and mechanical properties, an organic-inorganic hybrid nanocomposite based on modified halloysite nanotubes (mHNTs) and polyurethane was prepared. The HNTs were modified with an amino-silane coupling agent (KH550) and then reacted with polypropylene glycol, 2,2-Dimethylol propionic acid, and Toluene diisocyanate to form mHNTs/PU aqueous dispersions. The structure of the siloxane functionalized mHNTs was confirmed by a Fourier transform infrared study. The PU/mHNTs composites were characterized by using differential scanning calorimetry, scanning electronic microscopy, thermal gravimetric analysis, a tensile test, particle size analysis, and a water swelling experiment. The tensile strength, Young's modulus, and elongation at the break of the composite polymer with 0.5 wt % mHNTs was shown to be significantly improved, by approximately 200%, 200%, and 30%, respectively. An excess amount of mHNTs could weaken the reinforcing effect and stability of the composite emulsion. © 2016 Wiley Periodicals, Inc. J. Appl. Polym. Sci. **2016**, *133*, 43949.

KEYWORDS: clay; composites; films; polyurethanes

Received 27 January 2016; accepted 19 May 2016
DOI: 10.1002/app.43949

INTRODUCTION

Polyurethane has excellent toughness, abrasion resistance, and low temperature impact resistance,[1–3] and therefore it is widely used in flexible film and coating applications. In recent years, waterborne polyurethane (WPU) has gained attention because it is an environmental friendly material that meets the requirements of a minimum volatile organic component (VOC). However, WPU has some drawbacks, such as poor mechanical properties and weak water-resistance, which inhibit its extensive application. Also, during the preparation of polyurethane dispersion, the viscosity and stability of the prepolymer must be balanced at the expense of higher molecular weight, which directly causes inferior chemical resistance and mechanical properties in comparison to solvent polyurethane. Therefore, it is still necessary to identify a process for developing WPU with excellent properties.

Improvements in WPU are normally achieved with postcuring reactions[4] or polymer hybridization,[5–7] which enhances the molecular weight, cross-linking density, and performance properties. However, the postcuring reaction needs a curing agent for the PU dispersion, which inevitably raises the cost of the modification and operational requirement. The polymer hybridization simultaneously complicates the multistep fabrication process. Recently, organic/inorganic composites have attracted extensive attention because inorganic additives can offer excellent mechanical and thermal properties to polymers.[8–12] Some studies[13,16–18] have shown that significant improvements in thermal, mechanical, and flammability properties were obtained by the addition of a small quantity of nanoparticles to solvent-based polyurethane. Song *et al.*[18] treated multiwalled carbon nanotubes (MWCNTs) with Toluene diisocyanate (TDI), and then the TDI-modified MWCNTs were added to the polyurethane as curing agent; this connected the MWCNTs and polyurethane by chemical bonds. They found that surface-modified MWCNTs reinforced with a PU composite coating had the highest coefficient of friction and the highest wear resistance compared with a MWCNTs/PU composite created by a direct mixing method. However, demanding conditions and/or sophisticated procedures during the preparation of the MWCNTs were often required, which limits their commercial application because of the difficulty and cost of large-scale fabrication. Halloysite nanotubes (HNTs), a naturally occurring clay mineral, have been used as reinforcing nanoparticles because of their high aspect ratio, low percolation volumetric fraction, and chemical structure.[13–15] In order to obtain the best performance of the nanocomposites, the nanotubes should be well dispersed without becoming entangled or forming bundles.[16] However, the high surface area of the nanoparticles results in high reactivity and a strong tendency towards agglomeration. The

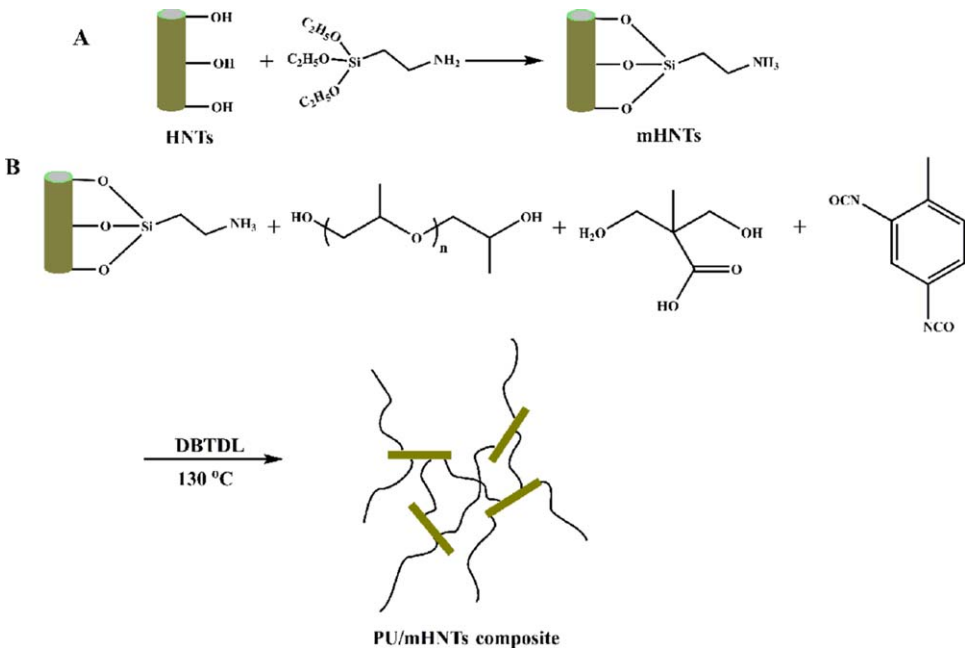

Scheme 1. Schematic for preparation of PU/mHNTs composite. [Color figure can be viewed in the online issue, which is available at wileyonlinelibrary.com.]

agglomeration of nanoparticles would seriously weaken the cohesive force between the polymer and the particles. Therefore, discovering how to improve the dispersion of nanotubes in a PU matrix is one of the most important factors for elevating the properties of composite polymers. Moreover, unlike the case with solvent-based polyurethane, the stability of polyurethane dispersion is mainly dependent on ionic groups in polymer chains. Therefore, the dispersion of HNTs in WPU and the preparation of stable HNTs/polyurethane composite emulsions could be new problems. Little work has been reported on the effects of nanotubes on the stability and thermal and mechanical properties of aqueous PU dispersion.

In order to design WPU with excellent water resistance and mechanical properties, an organic-inorganic hybrid nanocomposite based on HNTs and polyurethane is developed in this research (Scheme 1). Specifically, the HNTs were modified with 3-aminopropyltriethoxysilane (KH550). Then, the WPU emulsions containing the reactive mHNTs were synthesized by *in situ* polymerization. The modified mHNTs were used as a material in the preparation of polyurethane dispersion. mHNTs could be reacted with isocyanate and easily dispersed in the emulsions. The effect of the concentration of mHNTs in the PU matrix on the mechanical properties of the mHNTs/WPU composites is investigated in this work.

EXPERIMENTAL

Materials

N 220 (Polypropylene glycol, M_n 2000 g/mol), N 330(Polypropylene glycol, M_n 3000 g/mol) were dried at 120 °C under1–2 mmg H_g for 2 h before use. 2,2-Dimethylol propionic acid (DMPA) was dried in a vacuum oven for 2 h at 120 °C. Dibutyltin dilaurate (DBTDL), triethyl amine (TEA), acetone, toluene were used after dehydration with 4-A molecular sieves for 1day. Halloysite nanotube (HNTs), with an outer diameter between 15 and 100 nm and approximate length of 500–1000 nm, were obtained from Zhengzhou Jinyangguang China Clays Company (China). Silane coupling agent (KH550) was purchased from Aladdin company (America). TDI, distillated deionized water, absolute ethanol were used as received.

Preparation of Silane Coupling Agent Modified Halloysite Nanotubes (HNTs)

Halloysite nanotube (HNTs) was dried at 120 °C in vacuum oven. HNTs (5.0 g) and KH550 (10.0 mL) toluene (100.0 mL) were placed into a flask. Then, the mixture solution was ultrasonic dispersed for 1 h and stirred at 130 °C (as scheme 1). After 24 h, the resulting modified mHNTs were filtered and washed with absolute ethanol for three times. Finally, amino-functionalized mHNTs was obtained after drying in vacuum at 60 °C for 6 h.

Preparation of Polyurethane/Nanotubes Composite Emulsion

Polypropylene glycol, DBTDL, DMPA were poured into three-necked round bottom flask and the calculated amount (0, 0.5, 1, 2 wt % with respect to Polypropylene glycol) of KH550 modified mHNTs was dispersed in it for 0.5 h by using an ultrasonic bath. TDI was added into this mixture (NCO/OH = 1.3) and temperature was raised up to 90 °C until the theoretical NCO % reached (as Scheme 1). The change in the NCO value during the reaction was determined with the standard dibutylamine back-titration method (ASTM D 1638). The reactor was cooled down to below 40–50 °C and then freshly dried acetone was added to adjust the viscosity of these PU prepolymer. The prepolymer was neutralized by TEA and then distilled water was added to the mixture with vigorous stirring (1000 rpm) to obtain stable composite emulsion.

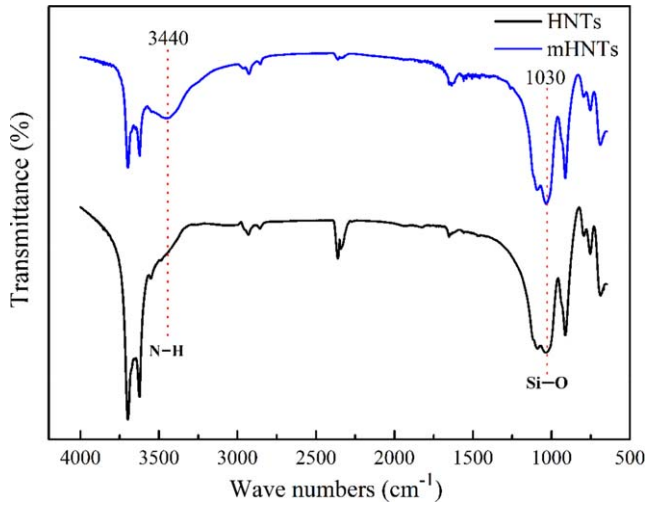

Figure 1. FT-IR spectra of HNTs and KH550 modified HNTs. [Color figure can be viewed in the online issue, which is available at wileyonlinelibrary.com.]

Characterization

Thermogravimetric analysis (TGA) was performed from 20 °C to 700 °C with a heating rate of 20 °C/min by using Q-500 (TA Instruments) under nitrogen atmosphere. The thermal properties of the samples were studied by using a differential scanning calorimetry (DSC) (NETZSCH, Germany) at a heating/cooling rate of 10 °C/min between −80 °C and 200 °C under nitrogen atmosphere. In order to homogenize the thermal history of the samples, a heat–cool–heat cycle was applied and the thermal transitions were analyzed based on the second heating scans.

Scanning electron micrographs (SEM) observation was carried out on a JSM-5900LV microscope (Japan). The films were broken in liquid nitrogen and the fracture surface of films was observed.

The tensile strength, elongation at break, and Young's modulus of PU and its composites were measured by an electronic universal tensile testing machine according to GB/T1040.3-2006 standard with 50 mm/min extension rate. The thickness of each strip was measured by a digital micrometer. In all cases, at least five samples were tested.

The nanotubes/PU composite emulsion was diluted with deionized water to 0.6% (wt %, solids) in the cell. The Z-Average diameter was measured at 25 °C by Zetasizer Nano S90 (Malvern).

The films were dried for 7 days at ambient temperature and sequentially heated at 80 °C for 4 h. The water absorption property was measured by immersing dried films in deionized water at 25 °C for 24 h. The films were then taken out of the water, and after wiping off the residual water on the surfaces using filter paper, their mass was recorded as m_1 and water absorption percentage was calculated by the following equation:

$$swell(\%) = \frac{m_1 - m_0}{m_0} \times 100\%. \quad (1)$$

where m_0 was the weight of initial dried film, and m_1 was the weight of swelled film.

RESULTS AND DISCUSSION

FT-IR Spectra of PU And PU/Nanotubes Composite Films

The KH550 modified halloysite nanotubes were used not only to improve reactivity with NCO-capped PU prepolymers, but also to elevate the dispersion in the polymer matrix. Figure 1 shows the FT-IR spectra of HNTs and mHNTs. The peaks at 3701 and 3620 cm^{-1} were attributed to OH stretching vibration, the peak around 2900 cm^{-1} was attributed to CH stretching vibration, the doublets at 1083 and 1030 cm^{-1} were attributed to in-plane Si-O stretching in the outer surface of HNTs, and the peak at 910 cm^{-1} was attributed to inner OH bending vibration.[17] Compared with the pristine HNTs, the mHNTs presented new absorbance peaks, such as an NH_2 stretching vibration band at 3440 cm^{-1}, and the peak at 1030 cm^{-1} that was exhibited sharply and narrowly after modification. These FT-IR spectra of transformation indicate that the silane coupling agent has been connected covalently to the outer surface of the HNTs.

TEM

Figure 2 shows the TEM micrographs of HNTs and KH550-modified HNTs (mHNTs). It can be seen that the HNTs tended to form aggregates into bundles [Figure 2(a)], whereas fewer bundles were observed in the mHNTs [Figure 2(b)]. This indicates that the dispersion of the HNTs was greatly improved after the HNTs were treated with KH550. This is because the HNTs treated with KH550 experienced a reduction of the Van der Waals force and a reduction in hydrogen bonding interaction among the mHNTs themselves.[17]

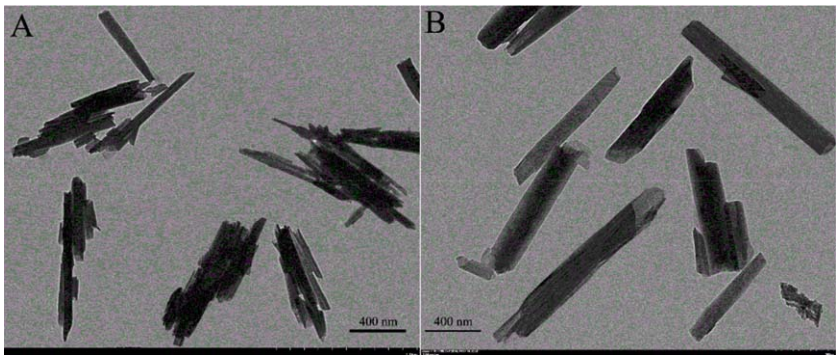

Figure 2. TEM micrographs of (A) HNTs; (B) mHNTs. [Color figure can be viewed in the online issue, which is available at wileyonlinelibrary.com.]

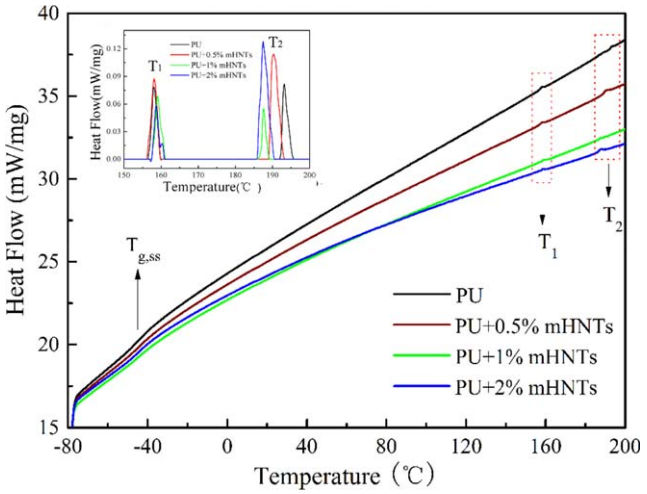

Figure 3. DSC curves of PU and PU/mHNTs composite. [Color figure can be viewed in the online issue, which is available at wileyonlinelibrary.com.]

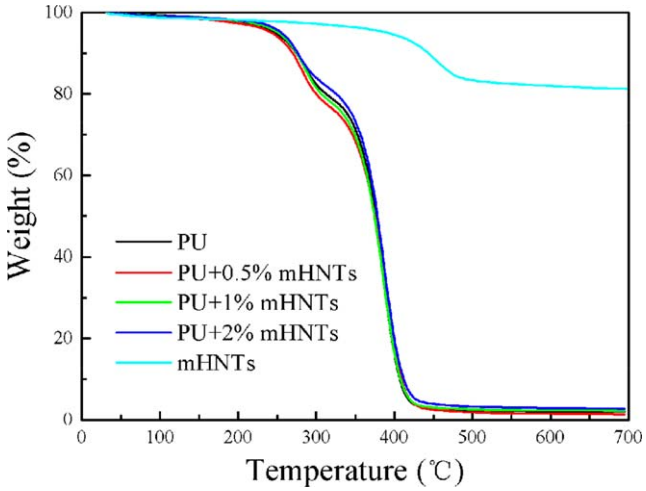

Figure 4. TGA curves of PU and PU/mHNTs nanocomposite. [Color figure can be viewed in the online issue, which is available at wileyonlinelibrary.com.]

Differential Scanning Calorimetry

The DSC curves of PU and PU/mHNTs composite films are shown in Figure 3. The glass transition temperatures of the soft segment ($T_{g,SS}$) presented at around −43 °C, and two tiny endotherm peaks were observed at 158 °C and 190 °C, respectively. The endotherm peak at 158 °C (T_1) was attributed to a hard segment long-range order of unspecified nature or to the onset of the microphase mixing of the hard and soft microphase.[19] However, the second endotherm peak occurring at 190 °C (T_2) was attributed to the melting of the hard segment microcrystalline region.[20] The values of the $T_{g,SS}$, T_1, and T_2 of all samples are shown in Table I. The small quantities of mHNTs used in the PU matrix have little influence on $T_{g,SS}$ and T_1 temperature, but the T_1 enthalpy reached its maximum with 0.5 wt % of mHNTs and subsequently decreased with the increase of mHNTs dosage. It was suggested that relatively more or larger long-range order hard microdomain can form in a soft continuous phase as 0.5 wt % mHNTs was added to the PU matrix, whereas if the order of this process was changed, then the microdomain would need more energy.[21] In addition, the T_2 temperature decreased with mHNTs dosage, suggesting that mHNTs could destroy the microcrystalline qualities of the hard microdomain. Thus, the mHNTs interact with hard segments instead of soft segments. However, the effect of mHNTs dosage on the hard microdomain could be related to the dispersion state of mHNTs in the PU polymer matrix. The appropriate content of mHNTs well dispersed in the PU matrix would be favorable to the formation of a center of hard segment aggregation, but if the excess weight of the mHNTs failed to distribute uniformly in the PU matrix, then the mHNTs would produce significant aggregation among themselves that would hinder the formation of hard long-order microdomains.[22] Similar results have been reported in other research.[21–24] Jelena *et al.*[24] prepared a ZnO/PU composite material and investigated the influence of ZnO nanoparticles on the thermal properties of the composite polymers. They found that the T_g of the nanocomposites was independent of the filler content, but the enthalpy of fusion increased with the amount of nanofiller content, confirming the interaction between the ZnO nanoparticles and the hard segments.

Table I. thermal Properties of the Nanocomposites from DSC Analyses

Sample	$T_{g,SS}$ (°C)	T_1 (°C)	$\triangle H_1$ (J/g)	T_2 (°C)	$\triangle H_2$ (J/g)
PU	−43.7	157.8	0.19	192.9	0.08
PU+0.5% mHNTs	−42.3	157.9	0.23	190.1	0.41
PU+1% mHNTs	−43.0	158.8	0.17	189.4	0.05
PU+2% mHNTs	−43.2	158.4	0.14	187.2	0.31

Thermogravimetric Analysis

TGA analyses were carried out to study the thermal degradation of the PU and PU/mHNTs composite films. Figures 4 and 5 show the weight loss and the first derivative of the weight loss (d*W*/d*T* or DTG) versus temperature, respectively. The thermal

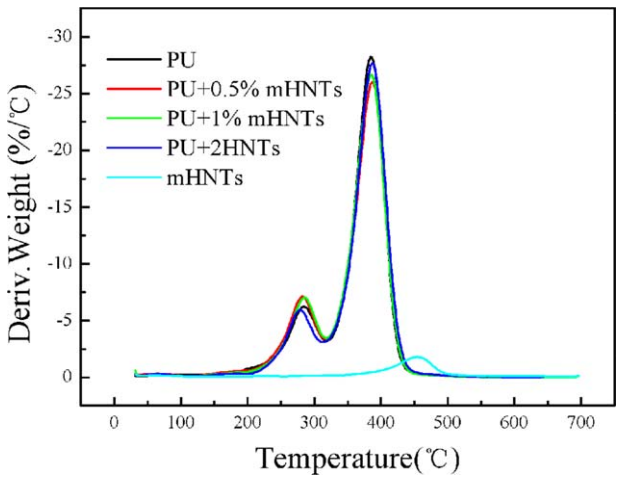

Figure 5. DTG curves of PU and PU/mHNTs nanocomposite. [Color figure can be viewed in the online issue, which is available at wileyonlinelibrary.com.]

Table II. Thermal Degradation Parameters of the Nanocomposites

Sample	Residue (wt %)	$T_{I,onset}$ (°C)	$T_{I,peak}$ (°C)	$T_{II,onset}$ (°C)	$T_{II,peak}$ (°C)
PU	2.06	254.1	284.3	318.8	385.2
PU+0.5% mHNTs	1.39	248.8	282.1	316.4	386.9
PU+1% mHNTs	2.26	252.7	285.1	319.2	385.2
PU+2% mHNTs	2.74	249.6	278.5	312.3	386.9

degradation of the films can be divided into two steps: the first weight loss could be attributed to the decomposition of urethane and urea linkages into isocyanate and alcohol with the possible formation of primary and secondary amines; the second weight loss could be attributed to the breaking of the polyol soft segments of the polyurethane.[24,25] The degradation onset temperature ($T_{I,onset}$) was approximately 250 °C, and the peak of DTG ($T_{I,peak}$), which indicates the point of maximum rate of change in the weight loss curve, was approximately 280 °C. In the second step, the values of these parameters ($T_{II,onset}$ and $T_{II,peak}$) were 316 °C and 386 °C, respectively. The values of T_{onset} and T_{peak} of each step are shown in Table II. It could be found that the values of $T_{1,onset}$ and $T_{1,peak}$ of the first step decreased with the addition of mHNTs, further implying that the mHNTs interact with the hard segments, resulting in a negative effect on the thermal stability and causing the urethane and urea bonds to break (on the hard segments).[24] These results indicate that the presence of mHNTs has little influence on the thermal stability of the PU because of the small quantity of mHNTs in the PU matrix.

SEM of PU And PU/mHNTs Nanocomposite

The fracture surfaces of the PU and PU/mHNTs composite films are shown in Figure 6. All samples exhibited a deeper and longer crack because of quick or brittle fractures in the liquid nitrogen, but the fracture surface of the 0.5 wt % mHNTs composite was quite different from the others: its fracture surface became rough and most of the longer cracks were disintegrated into a series of short cracks. The rough fracture surface indicates that there was a strong resistance to further propagation of cracks. Meanwhile, the rough fracture surface means that a large crack would encounter difficulties in propogating.[26,27] It is likely that this effect would improve the mechanical strength of the composite. However, when the dosage of mHNTs increased to 1 and 2 wt %, the fracture surfaces were unexpectedly similar to the PU film. This result was consistent with the DSC result, implying that the 0.5 wt % mHNTs dosage in the PU matrix is optimal for reinforcing the mechanical properties of PU dispersion.

Tensile Properties of PU/mHNTs Composite Films

Tensile tests were performed to evaluate the mechanical properties of the PU/mHNTs nanocomposites. Figure 7 shows the stress–strain curves of PU films prepared with different levels of mHNTs content. It can be seen that the mHNTs could reinforce the PU film effectively and that 0.5 wt % of mHNTs in the PU matrix produced the best mechanical properties among all of

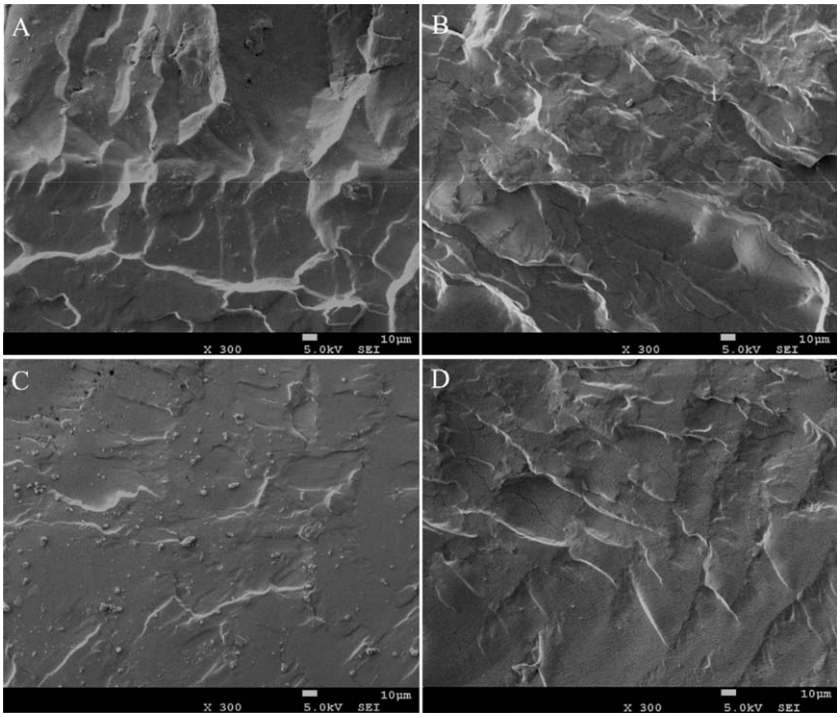

Figure 6. SEM pictures of PU and PU/nanotubes composite (A: PU; B: PU + 0.5 wt % mHNTs; C: PU + 1 wt % mHNTs; D: PU + 2wt % mHNTs).

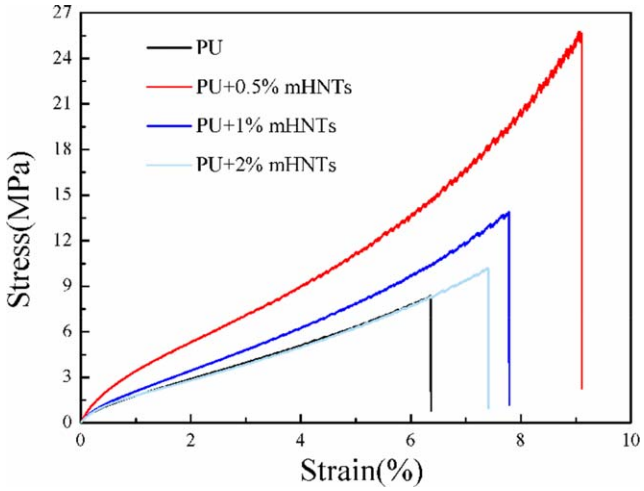

Figure 7. Tensile stress–strain curves of the composite films. [Color figure can be viewed in the online issue, which is available at wileyonlinelibrary.com.]

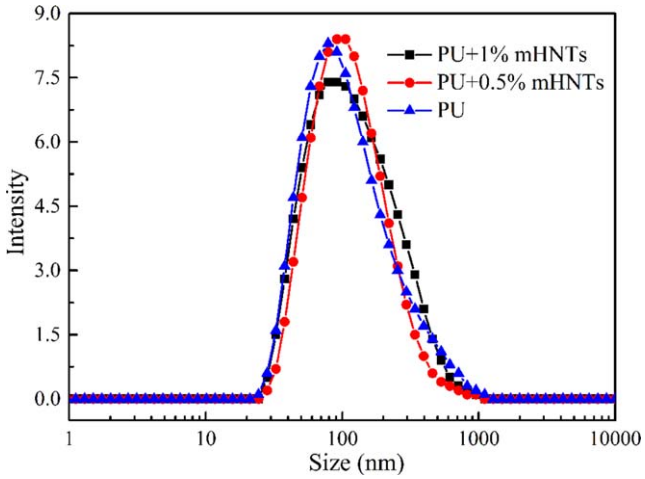

Figure 8. The influence of mHNTs dosage on particle size of composite emulsion. [Color figure can be viewed in the online issue, which is available at wileyonlinelibrary.com.]

the samples. The data regarding tensile strength, tensile modulus, and elongation at break of the PU and its composites are summarized in Table III. The results show that the characteristic parameters of the mechanical properties have been improved for all the composites. Moreover, the highest elasticity modulus and stress at break of the mHNTs/PU composite was achieved when the content of mHNTs was 0.5 wt %. The tensile stress of the mHNTs/PU nanocomposites increased from 8.3 to 25.62 MPa, and the elasticity modulus of the mHNTs/PU nanocomposites increased from 1.51 to 4.83 MPa. However, when the content of mHNTs increased from 0.5 to 2 wt %, the mechanical properties of the composite films were greatly decreased. Similar results could be observed in the DSC and SEM, which revealed that 0.5 wt % mHNTs in the PU matrix could improve the microphase separation between soft and hard segments. The reason may be attributed to better dispersion and covalent modification. Dispersion was probably one of the critical factors. mHNTs must be homogeneously dispersed to the level of isolated mHNTs individually coated with polymer; this condition is imperative in order to achieve efficient load transfer to the HNTs network. The effects of poor dispersion can be seen in a number of systems when the content of mHNTs in the PU matrix is increased beyond the point where aggregation begins. This is generally accompanied by a decrease in strength and modulus. The covalent cross-linking also played an important role in reinforcing the mechanical properties. After the mHNTs linked to the PU with covalent bonds, the mHNTs had better interfacial strength; this could reinforce the composites by effectively transferring the stress among the mHNTs and the PU matrix. Moreover, it can be concluded that better reinforcement and toughness performance was achieved with the addition of mHNTs to the WPU matrix. This reinforcement mechanism may be governed by the double-network model mechanism, in which rows of connected nanotubes form a second network that superimposes on the molecular network. Upon extending the rubber matrix, the nanotubes will align in rows parallel to the direction of the applied stress, resulting in an inhomogeneous local deformation.[17]

The Particle Size and Water Absorption

Figure 8 shows the effect of mHNTs dosage on the particle size of the composite emulsions. The small weight of the mHNTs causes a slight growth in the particle diameter of the composite emulsions, but the diameter of the nanotubes/PU composite emulsion with 2 wt % mHNTs would sharply increase and fail to achieve stable particle size information. This is because the excess mHNTs could entangle and form bundles. Unlike the case with solvent borne polyurethane, the stability of WPU depends on ionic groups in polymer chains created by repulsive interaction. However, the aggregated mHNTs bundles have larger volume, if they were buried in the PU matrix as core, and it would cause the number of carboxylic groups on the surface of the composite latexes decreased, while the repulsion interaction of the ionic groups decreased; thus, the WPU with 2 wt % mHNTs had a significant increase in diameter and decrease in stability. The particle size, size distribution, and water absorption of all samples are shown in Table IV.

Table III. The Content of mHNTs Influence on Tensile Strength Properties

Name	Elasticity modulus (MPa)	Stress at break (MPa)	Elongation at break (%)
PU	1.51 ± 0.52	8.30 ± 1.05	636.25 ± 107.71
PU+0.5% mHNTs	4.83 ± 0.43	25.62 ± 8.86	910.42 ± 60.89
PU+1% mHNTs	2.52 ± 0.36	13.90 ± 2.77	778.47 ± 31.67
PU+2% mHNTs	1.81 ± 0.30	10.11 ± 2.13	740.69 ± 23.17

Table IV. Information of PU and PU/Nanotubes Composite

Name	Z-Average diameter (nm)	PDI	Water absorption (%)
PU	93.19	0.365	20.20
PU+0.5% mHNTs	109.70	0.444	15.60
PU+1% mHNTs	109.50	0.302	22.60
PU+2% mHNTs	1.29e[4]	9.428	64.00

Unexpectedly, it was found that the PDI of the WPU with 1% mHNTs was lower than that of the WPU with 0.5 mHNTs. These data reflect what the size distribution of the composite emulsion is after filtration. In fact, some small quantities of precipitation have been filtered before measurement, which caused the tiny difference of PDI among composite emulsions. The water absorption results were consistent with those of other testing experiments. The water resistance of the composite film with 0.5 wt % mHNTs was obviously improved because of the increased cross-linking with hard segments, whereas continuously increasing the mHNTs content in the PU matrix led to the increase of water absorption. It can be further inferred that a positive dispersion of mHNTs in the PU matrix would play an important role in the reinforcing effect on the composite film. When 0.5 wt % mHNTs was used, it could be well dispersed in the PU matrix, which caused the amino groups on the surface of the HNTs to react completely with the NCO-capped PU prepolymer. It also caused the composite film to have better water resistance, while more mHNTs used in the PU matrix resulted in higher water absorption. That was because the excess amount of mHNTs could aggregate into bigger bundles, thus decreasing the specific surface area and reducing the reactivity of amino groups on the surface of the mHNTs. Hence, surplus hydrophilic amino groups were buried in the inner part of the polymer, which caused higher water absorption as the amount of mHNTs increased. In addition, the aggregated mHNTs bundles were beneficial to form a porous composite film, which improved the diffusibility for water in the film.

CONCLUSIONS

In this article, an organic-inorganic hybrid nanocomposite based on halloysite nanotubes (HNTs) and polyurethane was prepared to improve the water resistance and mechanical properties of WPU films. HNTs was modified with an amino-silane coupling agent (KH550) and then reacted with polypropylene glycol, DMPA, and TDI to form mHNTs/PU aqueous dispersions. The increase in the temperature of the hard segment long-range order (T_1) and the enthalpy of fusion of the hard segment microcrystalline region (ΔH_2) indicate that the mHNTs interacted with the hard segments of the PU, which led to a decrease in the thermal decomposition temperature of the hard segments. The reinforcing effect of the mHNTs on the PU film was related to the dosage of mHNTs in the PU matrix. An excess amount of mHNTs added to the system could weaken the reinforcing effect and stability of the composite emulsion. It was found that with the incorporation of 0.5 wt % mHNTs, the tensile strength, Young's modulus and elongation at break reached higher values than in the other samples. This remarkable improvement indicates that simultaneous reinforcement and toughening effects occurred because of the complete dispersion of mHNTs in the PU matrix. To summarize, the introduction of mHNTs into WPU molecular chains was an effective way to improve the water resistance and mechanical properties of WPU films.

ACKNOWLEDGMENTS

This study was supported by the Natural Science Foundation of China (NSFC 51073101, 51503130), support plan of Science and Technology Department of Sichuan Province, China (No. 2012GZ0096) and Xiamen Southern Ocean Research Center Program (14GZP004NF04, 14GQT61HJ31). We also thank Dr. Yin Wang of The Johns Hopkins University for providing HNTs.

REFERENCES

1. Manvi, G. N.; Jagtap, R. N. *J. Dispersion Sci. Technol.* **2010**, *31*, 1376.
2. Chattopadhyay, D. K.; Raju, K. V. S. N. *Prog. Polym. Sci.* **2007**, *32*, 352.
3. García-Pacios, V.; Iwata, Y.; Colera, M.; Miguel Martín-Martínez, J. *J. Adhes. Adhes.* **2011**, *31*, 787.
4. Howarth, G. A. *Surf. Coat. Int. Part B Coat. Trans.* **2003**, *86*, 111.
5. Wang, X. R.; Shen, Y. D.; Lai, X. J.; Liu, G. J.; Du, Y. *J. Polym. Res.* **2014**, *21*, 367.
6. Cheng, R.; Zhang, C.; Wang, J. *Adv. Mater. Res* **2014**, *904*, 170.
7. Fu, C. Q.; Xu, M.; Yang, Z.; Lv, Q. G.; Shen, L. *Adv. Mater. Res.* **2013**, *690-693*, 1620.
8. Hu, J. K.; Li, L.; Zhang, S. W.; Gong, S. L. *J. Appl. Polym. Sci.* **2013**, *130*, 1611.
9. Osman, M. A.; Mittal, V.; Morbidelli, M.; Massimo, S.; Ulrich, W. *Macromolecules* **2003**, *36*, 988.
10. Luo, Z.; Hong, R. Y.; Xie, H. D.; Feng, W. G. *Powder Technol.* **2012**, *218*, 23.
11. Burgentzlé, D.; Duchet, J.; Gérard, J. F.; Jupin, A.; Fillon, B. *J. Colloid Interface Sci.* **2004**, *278*, 26.
12. Wang, W. C.; Jiang, F. D.; Jiang, Y.; Lu, Y. L.; Zhang, L. Q. *J. Appl. Polym. Sci.* **2012**, *126*, 789.
13. Marini, J.; Pollet, E.; Averous, L.; Bretas, R. E. S. *Polymer* **2014**, *55*, 5226.
14. Du, M.; Guo, B.; Jia, D. *Polym. Int.* **2010**, *59*, 574.
15. Deng, S.; Zhang, J.; Ye, L.; Wu, J. S. *Polymer* **2008**, *49*, 5119.
16. Ryszkowska, J.; Jurczyk, K. M.; Szymborski, T.; Kurzydlowski, K. *J. Phys. E* **2007**, *39*, 124.
17. Jiang, L.; Zhang, C.; Liu, M. K.; Yang, Z.; Tjiu, W. W.; Liu, T. *Compos. Sci. Technol.* **2014**, *91*, 98.
18. Song, H. J.; Zhang, Z. Z.; Men, X. H. *Eur. Polym. J.* **2007**, *43*, 4092.
19. Chen, T. K.; Shieh, T. S.; Chui, J. Y. *Macromolecules* **1998**, *31*, 1312.

20. Bajsic, E. G.; Rek, V.; Sendijarevic, V.; Frisch, K. C. *J. Elastomers Plast.* **2000**, *32*, 162.

21. Heck, C. A.; Dos Santos, J. H. Z.; Wolf, C. R. *Int. J. Adhes. Adhes.* **2015**, *58*, 13.

22. Lee, S. I.; Hahn, Y. B.; Nahn, K. S. *Polym. Adv. Technol.* **2005**, *16*, 328.

23. Wu, W.; Cao, X. W.; Zhang, Y. J.; He, G. J. *J. Appl. Polym. Sci.* **2013**, *130*, DOI: 10.1002/app.39179.

24. Pavlicevic, J.; Špírková, M.; Bera, O.; Jovicic, M.; Pilic, B.; Balos, S.*Compos. Part B Eng.* **2014**, *60*, 673.

25. Siyanbola, T. O.; Sasidhar, K.; Rao, B. V. S. K.; Narayan, R.; Olaofe, O.; Akintayo, E. T.; Raju, K. V. S. N. *J. Am. Oil Chem. Soc.* **2015**, *92*, 267.

26. Subramani, S.; Choi, S. W.; Lee, J. Y.; Kim, J. H. *Polymer* **2007**, *48*, 4691.

27. Wu, C. L.; Zhang, M. Q.; Rong, M. Z.; Friedrich, K. *Compos. Sci. Technol.* **2002**, *62*, 1327.